Antiviral Bioactivity of Resveratrol Against Zika Virus Infection in Human Retinal Pigment Epithelial Cells

Constanza Andrea Russo
Universidad de Buenos Aires Facultad de Ciencias Exactas y Naturales
Maria Florencia Torti
Universidad de Buenos Aires Facultad de Ciencias Exactas y Naturales
Agostina Belén Márquez
Universidad de Buenos Aires Facultad de Ciencias Exactas y Naturales
Claudia Soledad Sepúlveda
Universidad de Buenos Aires Facultad de Ciencias Exactas y Naturales
Agustina Alaimo
Universidad de Buenos Aires Facultad de Ciencias Exactas y Naturales https://orcid.org/0000-0002-8070-9620
Cybele Carina García (cygarcia@qb.fcen.uba.ar)
Universidad de Buenos Aires Facultad de Ciencias Exactas y Naturales https://orcid.org/0000-0002-6431-7176

Research Article

Keywords: Polyphenols, Resveratrol, Flavivirus, Zika virus, Retinal Pigment Epithelium, Antiviral activity

Posted Date: May 4th, 2021

DOI: https://doi.org/10.21203/rs.3.rs-447551/v1

Version of Record: A version of this preprint was published at Molecular Biology Reports on July 20th, 2021. See the published version at https://doi.org/10.1007/s11033-021-06490-y.

Abstract

Resveratrol (RES) is a polyphenol with increasing interest for its inhibitory effects on a wide variety of viruses. Zika virus (ZIKV) is an arbovirus of the *Flaviviridae* family for which there is no approved treatment or vaccine, and which has become a major global health threat. Within the broad spectrum of ophthalmological manifestations after infection, retinal pigment epithelial cells (RPE) type is one of the most permissive and susceptible to the virus. This work explored the protective effects of RES on ZIKV-infected human RPE cells. RES treatment resulted in a significant reduction of infectious viral titer in infected male ARPE-19 and female hTERT-RPE1 cells. This protection was positively influenced by the action of RES on mitochondrial dynamics, restoring the ZIKV induced fragmentation of mitochondrial network to conditions similar to those of uninfected control cultures. Also, docking studies showed that RES has a high affinity for two enzymes of the rate-limiting steps of pyrimidine and purine biosynthesis and viral polymerase. In conclusion, our findings indicated that RES could be considered as an antiviral agent to treat ZIKV-induced ocular abnormalities.

Highlights

- ZIKV infects human Retinal Pigment Epithelial (RPE) cells.
- Resveratrol (RES) presents antiviral activity against ZIKV.
- RES mitigates the ZIKV-induced cytopathic effect on RPE.
- RES restores the ZIKV-induced mitochondrial network morphology disruption.
- RES exhibits an efficient binding affinity for enzymes of the rate-limiting steps of pyrimidine and purine biosynthesis and viral polymerase.

1. Introduction

Nature is an inexhaustible source of bioactives. At the present time, there is growing trend of returning to a natural medicine which has been used throughout thousands by different civilizations. As consequence, an increase in the demand to find natural bioactive substances with therapeutic properties with the aim to replace synthetic compounds results mandatory [1]. In line with this, various natural bioactive molecules with beneficial properties for health have been isolated and identified, which forces modern medicine to a paradigm change [2]. Notably, this century has been witness of a innovation in natural polyphenolic bioactives due to their myriad of benefits for health (e.g. neurodegenerative disorders) [3, 4].

Polyphenols have been of interest to researchers around the world as potential antiviral agents due to their low toxicity profile and high abundance in nature. So far, more than 10,000 polyphenols have been identified, among which resveratrol (RES) exhibits increasing attention [3].

RES (3,4',5-trihydroxystilbene) natural phenolic compound that occurs as both *trans* and *cis* isomers. The stilbene-based structure of RED comprises two phenolic rings connected by a styrene double bond. RES is

mainly found in red wine, skin of red grapes, bilberries, blueberries, cranberries, dark chocolate, pistachios, peanuts, and seeds [5, 6] . Polyphenols were postulated to have antiviral properties [7], and RES is not the exception. In particular, there are reports indicating that RES exerts inhibitory effects on a broad variety of viruses like influenza A, herpes simplex type 1, rotavirus, Middle East respiratory syndrome coronavirus (MERS), severe acute respiratory syndrome coronavirus 2 (SARS-CoV-2), dengue (DENV) and Zika (ZIKV) [8–16].

ZIKV is an arbovirus that consists of an enveloped, positive-sense, single-stranded RNA. Like DENV, yellow fever, West Nile, Japanese encephalitis and tick-borne encephalitis viruses, ZIKV is member from the *Flaviviridae* family [17]. They are transmitted to humans by *Aedes* (subgenus *Stegomyia*) mosquitoes; They are transmitted to humans by *Aedes* (subgenus *Stegomyia*) mosquitoes; nevertheless, human to human transmission might also occur via sexual contact, vertically from mother to foetus and via blood transfusion [18]. In 1947, in the Zika forest of Uganda, ZIKV was primarily identified in a sentinel rhesus monkey and was first detected in humans in 1952. In 2014, the virus quickly spread into the Americas and in 2016, the World Health Organization (WHO) declared ZIKV epidemic as a public health emergency [17, 19–21]. Considerable scientific efforts resulted in many candidate vaccines that are currently undergoing further clinical development. Nevertheless, nowadays there is no treatment or vaccine approved with a proven efficacy [21–23]. In Americas, ZIKV infection has been associated with a congenital syndrome characterized by severe central nervous system defects and also Guillain–Barré syndrome in adults [23]. Particularly, ocular involvement in ZIKV infection could occur in both infants and adults as congenital and acquired diseases, respectively. The wide spectrum of ophthalmological manifestations include conjunctivitis, optic nerve hypoplasia, optic disc pallor, more curved optic disc, retinal pigmentation changes, haemorrhagic retinopathy, and abnormal retinal vasculature, among others [24–26]. In addition, *in vitro* and *in vivo* studies revealed that Müller, retinal endothelial and retinal pigment epithelial (RPE) cell types resulted to be the most highly permissive and susceptible to ZIKV infection [27–30].

The RPE is a specialized monolayer situated in the interface between the neuroretina and the choriocapillaris where it forms the outer blood-retinal barrier. The RPE plays various physiological roles that are critical to retinal homeostasis, such as: nutrients and ions transport, light absorption, recycling compounds associated with the visual cycle, phagocytosis photoreceptor outer segments, immune modulation, and trophic factors secretion, among others. Hence, the RPE is vital for photoreceptor survival and visual function [31]. The occurrence of viruses or bacteria in RPE cells has been detected in animals and humans. Additionally, pathogen replication and toxin production can trigger RPE cell death. Accumulating evidence suggest that pathogen-induced chronic infection could be a risk factor in the aetiology of retinal disease, like age-macular degeneration [32]. Importantly, it has been suggested that RES treatment might exert positive effects in several ocular pathologies [33].

Although there is knowledge about the clinical manifestations at the ocular level, the amount of scientific background related to the intracellular steps of ZIKV in retinal cells, as well as potential new treatments with natural compounds, remains poorly studied. Therefore, the aim of the current study was to explore

the potential anti-ZIKV bioactivity of RES in human RPE cells from female and male origin by paying particular attention to the mitochondrial morphology status.

2. Materials And Methods

2.1. Biological and chemical reagents

2.1.1. Cell lines

ARPE-19 (ATCC®, CRL-2302TM) (karyotype XY) and the human-Telomerase Reverse Transcriptase immortalized RPE cell line (hRPE-1, ATCC® CRL-4000TM) (karyotype XX) were cultured in DMEM (GIBCO) supplemented with 2 mM L-glutamine, 100 IU / ml penicillin, 100 µg / ml streptomycin, 2.5 µg / ml amphotericin and 10 % fetal bovine serum (FBS) (Sigma-Aldrich) [6, 34].

African green monkey kidney epithelial cells (Vero, ATCC®, CCL-81TM) were cultured in minimal Eagle essential medium (MEM, GIBCO) supplemented with 100 µg / ml gentamicin, 100 µg / ml streptomycin and 5 % FBS [21].

2.1.2. Virus

ZIKV Argentine isolated INEVH116141 (ZIKV-AR) (Instituto Nacional de Enfermedades Virales Humanas (INEVH) Pergamino, Argentina) [21]. All work was performed under strict level 2 biosafety working conditions. Infection protocols were approved by the Office of Environmental Health and Safety at the IQUIBICEN-UBA-CONICET.

2.1.3. Chemicals

trans-RES (RES) (3, 5, 4'-trihidroxi-trans-estilbeno) (purity > 99% from Zhejiang Chempharm was provided by Temis Lostaló SA [35]. RES stock of 5 mM was prepared by dissolving the drug in a mixture of 40 % v/v ethanol (EtOH) and 60 % v/v phosphate-buffered saline (PBS). Other chemicals used were of analytical grade.

2.2. Cell viability assay

Cell viability was assessed by MTT assay (Sigma-Aldrich) reduction assay as previously described [35]. Absorbance measurements were performed with an ELISA reader (BIO-RAD).

2.3. Viral infection

ARPE-19 or hRPE-1 cells were grown in 24-well plates. After the medium was removed, 100 µl of a dilution of the viral stock in PBS were inoculated to infect with a multiplicity of infection (MOI) of 0.5 for 1 h at 37°C/ 5 % CO_2, moving the plate every 20 min. Afterwards, the inoculum was removed and 500 µl of culture medium was placed in the presence or in the absence RES for 48 h [34].

2.4. Immunofluorescence assay (IFA)

Cells were fixed with 4% paraformaldehyde, permeabilized with 0.25% Triton X-100-PBS (10 min, RT) washed with PBS and incubated in 1% bovine serum albumin -PBS for 30 min at RT. Cells were incubated with primary anti-bodies rabbit polyclonal anti-TOM-20 at 1:500 (Santa Cruz Biotechnology, Inc.) and mouse monoclonal anti-E at 1:300 (Abcam, ab155882) for 1 h at 37 ° C. After washing, cells were incubated with the mixture of secondary antibodies: anti-rabbit IgG Alexa Fluor 488 and anti-mouse IgG Alexa Fluor 555 at 1:1000, for 1h at 37 ° C. Then, washed samples were incubated with DAPI during 10 min for nuclei labelling. Finally, samples were analysed with an Olympus IX71 epifluorescence microscope and with an Olympus FLUOVIEW FV1000 (Olympus Corporation). Image co-location analysis was performed using the ImageJ (NIH) program. One-hundred cells *per* sample were quantified and categorized as cells displaying tubular or fragmented (rounded and globular) mitochondria agreeing to Alaimo *et al.*, [35, 36] with slights modifications.

2.5. Viral yield determination

Serial 10-fold dilutions were made from ZIKV-infected cell supernatants in PBS. Samples were used to infect Vero cells using 100 µl / well of each dilution. Cells were incubated for 1 h at 37°C and shacked every 20 min. Subsequently, the inoculum was removed and washed. Cells were covered with 1 ml of semi-solid medium (MEM 1 % methylcellulose) and incubated at 37 ° C for 3 days. Then, cells were fixed with 10 % formaldehyde for 10 min, washed and stained with 0.1 % crystal violet in 20 % ethanol. Plaques were counted, and viral yield determined.

2.6. Bioinformatics analysis

2.6.1. Homology modelling of ligand binding site domain of AHR

Amino acid FASTA sequence of AHR was downloaded from Protein Database (Protein ID: NP-001612.1). Amino acid residues of the ligand binding site domain of AHR were selected (272-389). The modelling of the 3Dstructure of the domain of AHR was performed by the homology modelling program SWISS-MODEL [37–41]. By using ProMod3, models were built based on the target-template alignment. Template search with BLAST and HHBlits has been assessed against the SWISS-MODEL template library. Coordinates were copied from the template to the model. Insertions and deletions were remodelled by using a fragment library and then, side chains were rebuilt. The geometry of the resultant model was regularized by applying a force field. The best homology model was selected according to Global Model Quality Estimation (GMQE) and Qualitative Model Energy Analysis (QMEAN) statistical parameters. Model quality and validation were performed using PROCHECK [42], Verify3D [43] and ProSA [44]. Further, docking of known ligands, the agonist TCDD (2,3,7,8-tetrachlorodibenzodioxin) and the antagonist CH-223191 [45] was done.

2.6.2. Molecular docking

3D ligand structures were drawn using Avogadro2 1.93.0 [46]. The ligands were optimized at semi-empirical PM6 calculations using Gaussian09 [47] and the pdb files were generated by Molden [48]. The following protein crystal structures were obtained from RCSB Protein Data Bank (PDB): Zika NS5 polymerase domain (RdRp) (PDB ID: 6LD5), guanosine 5'-monophosphate oxidoreductase 2 (GMPR2) (PDB ID:2C6Q) dihydroorotate dehydrogenase (DHODH) (PDB ID: 6CJF), and CYP1B1 (PDB ID:3PM0). Ligands and water molecules were deleted from the original protein. Ligands were re-docked into the active site of each protein as a method of re-validation. RES was docked into the active site of the proteins. Molecular docking was performed by AutoDock 4.2.6 software. Protein and ligand structures were managed before molecular docking studies using AutoDock Tools 1.5.6 (Scripps Institute, La Jolla, CA, USA). Gasteiger charges were incorporated into the proteins and atoms were assigned to AD4. For each protein, the AutoGrid program was used to create a grid box to cover the active site of the proteins. Docking simulations were performed using the Lamarckian genetic algorithm (LGA). A total of 300 runs along with 5.10^6 energy evaluations and 1.10^5 iterations were carried out. Docked poses were chosen based on scoring functions. Protein-ligand docked complex structure was visualized using UCSF Chimera [49] and the LigPlot+ v.2.1 software was used to study 2D protein-Res interactions.

2.7. Statistical analysis

Experiments were carried out in triplicate. Results are expressed as mean ± SD values. One-way or two-way ANOVA were applied followed by the Newman-Keuls a *posteriori* test. Results were considered significant at $p < 0.05$ (GraphPad Prism 6.01 software).

3. Results

3.1 Effect of RES on ZIKV-infected RPE cell lines

RPE are highly permissive to ZIKV replication. To explore the antiviral activity of RES against ZIKV in a retinal cell model, we employed ARPE-19, which is a spontaneously arising RPE cell line of male origin that retains normal karyology [50] and hTERT-RPE-1 (from now on, abbreviated hRPE-1), which is a near-diploid human cell line of female origin [51]. both cell lines maintain the morphology and functions of *in vivo* human RPE cells [52].

First, we assessed by MTT reduction test the cytotoxicity effect of different concentrations of RES (5 - 250 µM) on ARPE-19 and hRPE-1 cell lines. **Figure 1a-b** denote that RES concentrations higher than 100 µM significantly reduced cell viability ($p < 0.01$ vs control), while at lower concentrations there were no significant differences in both cell lines. In accordance with the results obtained, we decided to work with 25 - 50 µM of RES.

Then, we explored the antiviral effects of RES on ZIKV replication. ARPE-19 and hRPE-1 cell lines were infected with ZIKV and following viral adsorption, cell cultures were incubated in the presence or absence of 25 or 50 µM RES. After 48 h of infection, cell morphology was analysed. **Figure 1c-d** shows that ZIKV caused an evident cytopathic effect (CPE) such as cell rounding and lysis. Both cell lines used were

equally susceptible to the infection along with the fact that presented similar CPE degrees. The addition of 50 μM RES attenuated the CPE in ARPE-19 and hRPE-1 cell lines not only similarly, but also these cells exhibited equivalent morphologies to the cell control cultures **(Figure 1c-d)**.

To evaluate whether the RES-protective effect during ZIKV infection was due to an *in vitro* inhibition of viral replication, we quantified by standard plaque assay the impact of the RES treatment on the viral particle production obtained in the supernatant of these cell cultures. As it can be observed in **Figure 1e**, in ARPE-19 cells the treatment with 25 and 50 μM RES reduced 44 % and 72 % of viral titer, respectively ($p < 0.001$). Similarly, 25 and 50 μM RES decreased the production of infectious viral particles by 29 % and 75 %, respectively ($p < 0.001$) in hRPE-1 cells **(Figure 1f).** Remarkably, viral production was similar in both cell models, without significant differences in the obtained viral yield (6-7 x 10^3 UFP/ml); however, 25 μM RES was more effective in terms of reducing the viral titer in ARPE-19 in comparison to hRPE-1, while 50 μM RES inhibited the viral titer in an equivalent effective manner in both cell lines. Hence, we decided to carry out next experimental assays with 50 μM RES.

Our results suggested that RES presented a protective role for the RPE cells against ZIKV, since inhibited viral replication and cellular damage.

3.2 Effect of RES on mitochondrial dynamics in ZIKV-infected RPE cells

RES impact rigorously depends on its concentration in both *in vitro* and *in vivo* models. That is, at concentrations less than 50 μM, RES exerts antioxidant and cell death protection. In counterpart, RES > 50 μM promotes unstable redox environment, rise cytotoxicity, as well as mitochondrial potential membrane loss and apoptosis [53]. Mitochondria are greatly dynamic organelles that move continuously along the cytoskeleton and remodel their morphology by the antagonistic processes of fusion and fission in accordance with cellular demands. The mitochondrial dynamics (DM) process is highly regulated and links the fate of the mitochondria and the cell [36, 54]. The sensitivity of DM to subtle physiological alterations in the cellular redox environment makes it an interesting event to study in relation to the mechanism of an antiviral compound [55]. In addition, we recently proved that ZIKV infection alters the balance of DM towards the fission process in RPE cells [34]. Hence, RPE cell cultures were infected with ZIKV, incubated in the presence or absence of 50 μM RES and after 48 h post infection (p.i.) immunofluorescence assay was performed. Regarding mitochondrial morphologies, as can be seen in **Figure 2a-b,** in non-infected RPE cells these organelles presented mostly long tubular shape; however, under ZIKV infection conditions, RPE cells shown rounded, swollen, and fragmented mitochondria. Notably, ZIKV-infected RES-treated cells exhibited mitochondrial morphologies similar to non-infected cells.

A detailed observation under confocal microscope allowed the quantification of the mitochondrial morphologies in each sample. Selected images of non-infected (data not shown), ZIKV-infected **(Figure 3a)** and ZIKV-infected RES-treated **(Figure 3b)** were reconstructed in 2D and 3D with Fiji imaging software by applying “3D Volume” in order to analyse mitochondrial morphologies. In non-infected ARPE-19 cell

line (Mock) 90 % of mitochondria were found tubular and only 10 % of the cells showed mitochondria with a fragmented shape (data not shown). As expected, in the ZIKV-infected cultures these percentages were significant modified. Only 35 % of the cells presented mitochondria showing tubular morphology ($p < 0.001$). Finally, in ZIKV-infected RES-treated cells, 54% of the population presented tubular morphologies. The latter values were significantly different in comparison with the infected ($p < 0.05$) and non-treated conditions ($p<0.01$) **(Figure 3c)**. In accordance, non-infected hRPE-1 cell line showed 86 % of mitochondria with tubular morphology and only 14 % fragmented (Mock), but in ZIKV-infected samples the percentages changed to 35 % of tubular and 65 % fragmented mitochondria ($p < 0.001$). Moreover, RES restored the tubular morphologies in 79 % of the cells ($p < 0.01$) in ZIKV-infected cells. Notably, these samples completely restored the rate of tubular mitochondria ($p < 0.05$) **(Figure 3d)**.

Collectively, results evidenced that RES reversed ZIKV-induced mitochondrial morphology disruptions.

3.3 Mechanism of action of RES against ZIKV infection

To gain some insights on the antiviral mechanism of action of RES, we applied modelling and docking studies of known and potential RES cellular and viral targets [56]. Particularly, it is well described that RES inhibits the cytochrome P450, family 1, subfamily B, polypeptide 1 (CYP1B1) expression by preventing the binding of the aryl hydrocarbon receptor (AHR) to promoter sequences that regulate CYP1A1/CYP1B1 transcription [45, 57–60]. It was suggested that RES might have a direct action on AHR [61]. Importantly, we recently showed that during ZIKV and DENV infection, AHR transcriptional targets CYP1A1 and CYP1B1 enhanced their expression. Also, we demonstrated that AHR is a druggable pro-viral target for flaviviruses [23]. Certainty, this activity of RES might represent an important part of the inhibition of ZIKV replication but is not the only mechanism involved. RES also interferes with several phosphorylation signalling pathways, including those activated by protein kinase C (PKC) and by mitogen-activated protein kinases (MAPKs) [62]. Additionally, RES decreased adenosine triphosphate (ATP) hydrolysis activity of the ZIKV NS3 helicase *in vitro* [63]. The molecular docking and structural dynamics simulations revealed that RES stabilizes the P-loop and triggers the RNA-binding loop to block the RNA-binding pocket [64]. Thus diverse mechanisms of action are operating during the inhibition of ZIKV infection.

It has been extensively studied that mitochondrial enzymes of the rate-limiting steps of pyrimidine and purine biosynthesis like the dihydroorotate dehydrogenase (DHODH) and guanosine monophosphate reductase 2 (GMRP2) are essential for the multiplication of RNA viruses [65–69].

To explore if aforementioned relevant mitochondrial enzymes could also be targeted by RES, we used bioinformatics tools. We included the well-characterized RES target CYP1B1, jointly with AHR, DHODH and GMRP2. Moreover, we analysed the possibility of RES direct action on ZIKV NS5 RNA-dependent RNA polymerase (RdRp). We generated by homology the 3D structure of the ligand binding domain of AHR (PAS-B domain) using SWISS-MODEL server. This server was successful in generating the 3D structure using crystal structure of Heterodimeric CLOCK: BMAL1 Transcriptional Activator Complex (PDB ID: 4F3L) as the template. The QMEAN scoring function was -1.60 and the GMQE value was 0.66. Validation of the

model using Ramachandran plot available with PROCHECK revealed that 91.3 % residues were in the most favored regions, 7.6 % in allowed regions, 1.1 % in generously allowed regions and 0.0 % in the disallowed regions. The parameters plot statistics suggested that the quality of the predicted model was optimal. According to the Verify3D server, the quality factor of the AHR domain residues domain showed that the 94.29 % of the residues had an averaged 3D-1D score ≥ 0.2 which represents an optimal score. ProSA tool allowed to determine that the Z score for the model was -4.42, which is within the range of scores usually found for NMR derived structure for the native protein of comparable size. While the structure assessment reports were relatively good quality for the predicted structure of AHR domain, it was not subjected to loop refinement. The complex AHR domain and the well characterized AHR agonist 2,3,7,8-tetrachlorodibenzodioxin (TCDD) showed a binding energy of -8.36 kcal/mol and the complex AHR domain- and the commercial AHR inhibitor CH 223191, an energy of -9.21 kcal/mol.

The possible mechanisms involved in the activity of RES were carried out through a molecular docking study. The docking process was performed using AutoDock4. Firstly, for the validation of the molecular docking, a re-docking was executed with the co-crystallized ligands and was evaluated that the binding poses coincided. The poses of the co-crystallized ligands overlapped efficiently with the best poses of the docked ligands. Both 2D and 3D interactions protein-RES are represented in **Figure 4a, i-iv**. CYP1B1 is a known RES target, therefore its binding energy was considered as a reference [57, 70]. Furthermore, known ligands for each protein have been considered as positive controls: TCDD and CH-223191 for AHR, 4,5-dihydroorotic acid (DHO) for DHODH, guanosine monophosphate (GMP) for GMPR2 and ATP for RdRp. The binding energies are represented in **Figure 4b** and in **Table 1**. The affinity value of less than 5 kcal/mol depicts negligible binding; although values closer to 10 kcal/mol indicate effective binding [71].

The docking study revealed that RES exhibited a strong binding affinity (more than 5 kcal/mol) for each protein targets **(Table 1** and **Figure 4b)**. In all cases, the three hydroxyl groups of RES established hydrogen bonds with the protein residues. The most stable complex was RES-DHODH (-8.15 kcal/mol), even more stable than the complex RES-CYP1B1. Nevertheless, the control ligand (DHO) showed more affinity for DHODH (-8.35 kcal/mol). RES displayed three hydrogen bonds with the amino acid residues of DHODH, and ten residues were involved in hydrophobic contacts **(Figure 4a, ii)**. In the same way, eight of these amino acids, coincided with the amino acid that interacted with DHO **(Table 2).** On the other hand, the GMPR2-RES complex showed a binding affinity of -7.65 kcal/mol. The complex was less stable than CYP1B1-RES complex but more stable than GMPR2-GMP complex. The higher affinity of RES could be explained by the hydrophobic contacts, while RES interacted with GMPR2 by eleven amino acids, GMP only interacted with eight residues **(Table 2)**. The interactions involved in GMPR2-RES complex were three hydrogen bonds eleven hydrophobic contacts **(Figure 4a, iii)**. Residues Cys186 and Gly220 were also involved in the GMPR2-GMP complex **(Table 2)**. The AHR-RES complex had a binding energy of -7.42 kcal/mol, thus the affinity is lower than AHR-TCDD complex (-8.36 kcal/mol) and AHR-CH 223191 (-9.21 kcal/mol). The ligand displayed three hydrogen bonds with the residues Tyr39, Gly50 and Gln112, and ten residues of AHR were involved in hydrophobic contacts **(Figure 4a, i)**. Such as AHR-RES complex, AHR-TCDD complex interacted with eight amino acids **(Table 2)**. Finally, the RdRp-RES complex showed a binding energy of -7.45 kcal/mol. Although the affinity is lower than CYP1B1-RES, it is higher than ATP-

RdRp (-6.77 kcal/mol). Three RdRp amino acids were involved in hydrogen bond and eight residues were involved in hydrophobic contact **(Figure 4a, iV)**. In the same way, eleven of these amino acids were involved in the RdRp-ATP complex **(Table 2)**. Tyr768, Thr795, Thr796 and Ser798 made H-bonds with ATP and these bonds could be interrupted by the interaction with RES. In addition, RES has a higher number of hydrophobic contacts, which could explain its higher affinity.

Altogether these results suggested that DHODH, GMPR2 and RdRp are RES potential targets that should be considered as part of it anti-ZIKV action.

4. Discussion

Polyphenols include in their chemical structure one or more aromatic rings along with one or more hydroxyl groups linked to a benzene ring. The polyphenolic family can be categorized as flavonoids and non-flavonoids. Among the latter, are the stilbene subfamily, to which RES belongs [72–74]. In the last years, increased evidence suggests that RES may have a great potential in the treatment of several ocular pathologies [6, 8, 33, 75–78]. Indeed, RES was studied for antiviral effects related with inhibitions of viral replication, protein and acid nuclei synthesis and gene expression, for an amount of viruses involving, hepatitis C virus, influenza virus, human immunodeficiency virus, herpes simplex virus, human coronaviruses MERS and SARS-CoV-2 [11, 79, 80]. More recently, two synthetic RES derivatives showed anti-DENV activity targeting viral RNA translation and viral replication, which could demonstrate a potential antiviral effect against flaviviruses [81]. Additionally, RES was investigated for its ability to inhibit ZIKV replication *in vitro* in different cell lines using several treatment regimens. RES exhibited modest virucidal activity against ZIKV but showed antiviral activity in a dose-dependent manner. Interestingly, there was no substantial decrease in ZIKV titer when RES treatment was applied to cells prior to ZIKV infection, influencing that RES does not prevent viral infection [13].

In spite of this available information, there are no reports so far where RES has been evaluated as a treatment to combat viral infections in the eye. Thus, the present is the first work where the antiviral effect of RES is evaluated in *in vitro* ZIKV infections in two retinal cell lines with a male and female origin.

On the other hand, mitochondria are involved in a plethora of different functions such as the maintenance of cellular homeostasis, metabolism, innate immunity, cell cycle, cell death and other signalling pathways [55, 82]. The maintenance of a proper fusion and fission balance is critical for preserving healthy cells [54]. Mitochondrial dynamics could be disturbed by a several pathogens (e.g. bacteria and viruses) in order to impact their intracellular survival or elude host immunity[82]. Therefore, the relationship between mitochondrial dynamics and viral pathogenesis could be a platform to develop brand-new antiviral treatment strategies and/or drugs [83]. Reports describing the relationship between the flavivirus infection and alterations in mitochondrial dynamics are mainly focused on DENV. Notably, while the existing articles all conclude the existence of mitochondrial fission and fusion imbalance in infected cells, there are controversies over which process is favoured [84–86]. The formation of youthful

mitochondria (biogenesis) and the decline in mitochondrial ROS production significantly decrease cellular oxidative stress and inflammation, restore cellular energetics and limit cell death [87, 88].

In a recent report, we demonstrated that ZIKV-infected ARPE-19 and hTERT-RPE1 cells ZIKV exhibited a disbalance of mitochondrial dynamics toward fission [34]. As far as we know, there are no reports that interconnect any type of virus and the positive impact of polyphenols on mitochondrial dynamics. Even less, in the ocular context. Therefore, the present report is a pioneer in demonstrating that RES restored the ZIKV-induced fragmented mitochondrial network to conditions similar to control cultures (elongated, threadlike mitochondria homogeneously distributed throughout the cytoplasm). Of note, the major fluorophore of toxic lipofuscin (A2E), induced mitochondrial fission in ARPE-19; meanwhile, 25 μM RES significantly mitigate such effect [35]. Wang *et al.*, mentioned that mitochondrial health is essential to counteract age-related neurodegenerative diseases, including oculopathy. In aging zebrafish retinas (as a model for age-related oculopathy), authors proved that 10-days treatment with RES (20 mg/L) improve the dysfunctional mitochondrial fission-fusion dynamics [88]. In addition, RES (0.1, 1 and 10 μM) ameliorated the mitochondrial swelling and abnormal morphology in transformed retinal ganglion RGC-5 cells in an ocular hypertension model [89]. Finally, in a recent report, 4 μM RES positively influenced on mitochondrial dynamics in serum deprived-retinal neuronal R28 cells [90]. Our evidence, together with previous reports, suggest that RES would be a useful addition in ocular nutritional supplements against ZIKV or related flavivirus infection.

Regarding the mechanism of action of RES, the direct molecular target of this bioactive has been elusive. Viruses rely on specific host factors to complete their multiplication cycles. Purines and pyrimidines are important constituents of RNA and DNA. Therefore, inhibition of mitochondrial enzymes involved in nucleosides biosynthesis represents a successful antiviral strategy. The inhibition of GMPR2 can deplete guanine nucleotide pools, followed by a decrease in DNA and RNA synthesis [91]. Moreover, the DHODH is a rate-limiting enzyme in the de novo biosynthesis pathway of pyrimidines. Therefore, the inhibition of pyrimidines biosynthesis as a potential approach the treatment of many infectious diseases [92, 93]. Certainly, the predicted inhibition of GMP and DHODH mediated by RES reported in the present work suggests that these mechanisms contribute to the blockade of ZIKV replication.

Furthermore, RES has been reported as an activator of one of the mammalian forms of the sirtuin family of proteins (SIRT1) [94]. Interestingly, it has been proposed that SIRT1 exert a considerable role in ocular diseases by influencing a range of physiological and pathological events for instance angiogenesis, inflammation, oxidative stress and aging [95]. To note, multiple studies have explored the relationship between RES, sirtuins and viruses [96]. In this sense, the SIRT1/AMPK axis triggering by RES may also explain the improvement of mitochondrial physiology.

5. Conclusion

In this study, we report that RES inhibited the ZIKV-induced cytopathic effect on RPE and restored the ZIKV-induced mitochondrial network morphology disruption. Also, we provide new perspectives about the

mechanism of action of RES involving the interference in the binding of ligand of important cellular enzymes that are essential for viral replication **(Figure 5)**. In summary, our results showed *in vitro* bioactivities of RES against ZIKV, providing evidence to support further comprehensive assessments *in vivo* and the possible clinical advantages for the treatment of ocular infection by ZIKV.

Declarations

Funding

This report was supported by Universidad de Buenos Aires (UBA) (20020170100363BA), Consejo Nacional de Investigaciones Científicas y Tecnológicas (CONICET) PIP112201701001 71CO and Agencia Nacional de Promoción Científica y Tecnológica (ANPCyT), Argentina (PICT 2016-1151). CSS, AA, CCG are members of the Research Career from CONICET; ABM is fellow from CONICET and MFT was supported by PhD fellowship from ANPCyT.

Conflict of interest/Competing interests.

The authors declare that there is no conflict of interest.

Availability of data and material

Not applicable

Code availability

Not applicable

Authors' contributions

AA and CCG contributed conception and design of the study. CAR, MFT, ABM and CSS performed the experiments and analyzed data. All authors contributed to manuscript revision, read, and approved the submitted version.

Ethics approval

Not applicable

Consent to participate.

All authors have given their consent to participate in this report and submit it to *Molecular and Cellular Biochemistry*.

Consent for publication

All authors have approved consent to publish if accepted.

Acknowledgments.

We are grateful to all colleagues from our laboratories for helpful advice and discussions.

References

1. Yuan H, Ma Q, Ye L, Piao G (2016) The traditional medicine and modern medicine from natural products. Molecules 21:. https://doi.org/10.3390/molecules21050559
2. Tufarelli V, Casalino E, D'Alessandro AG, Laudadio V (2017) Dietary Phenolic Compounds: Biochemistry, Metabolism and Significance in Animal and Human Health. Curr Drug Metab 18:905–913. https://doi.org/10.2174/1389200218666170925124004
3. Cory H, Passarelli S, Szeto J, et al (2018) The Role of Polyphenols in Human Health and Food Systems: A Mini-Review. Front. Nutr. 5:87
4. Zhao D, Simon JE, Wu Q (2020) A critical review on grape polyphenols for neuroprotection: Strategies to enhance bioefficacy. Crit Rev Food Sci Nutr 60:597–625. https://doi.org/10.1080/10408398.2018.1546668
5. Gambini J, López-Grueso R, Olaso-González G, et al (2013) Resveratrol: Distribución, propiedades y perspectivas. Rev Esp Geriatr Gerontol 48:79–88. https://doi.org/10.1016/j.regg.2012.04.007
6. Buosi FS, Alaimo A, Di Santo MC, et al (2020) Resveratrol encapsulation in high molecular weight chitosan-based nanogels for applications in ocular treatments: Impact on human ARPE-19 culture cells. Int J Biol Macromol 165:. https://doi.org/10.1016/j.ijbiomac.2020.09.234
7. Kamboj A (2012) Antiviral activity of plant polyphenols. J Pharm Res 5:2402–2412
8. Hua J, Guerin KI, Chen J, et al (2011) Resveratrol inhibits pathologic retinal neovascularization in Vldlr-/- Mice. Investig Ophthalmol Vis Sci 52:2809–2816. https://doi.org/10.1167/iovs.10-6496
9. Palamara AT, Nencioni L, Aquilano K, et al (2005) Inhibition of influenza A virus replication by resveratrol. J Infect Dis 191:1719–1729. https://doi.org/10.1086/429694
10. Faith SA, Sweet TJ, Bailey E, et al (2006) Resveratrol suppresses nuclear factor-κB in herpes simplex virus infected cells. Antiviral Res. https://doi.org/10.1016/j.antiviral.2006.06.011
11. Abba Y, Hassim H, Hamzah H, Noordin MM (2015) Antiviral Activity of Resveratrol against Human and Animal Viruses. Adv Virol 2015:184241. https://doi.org/10.1155/2015/184241
12. Annunziata G, Maisto M, Schisano C, et al (2018) Resveratrol as a Novel Anti-Herpes Simplex Virus Nutraceutical Agent: An Overview. Viruses 10:. https://doi.org/10.3390/v10090473
13. Mohd A, Zainal N, Tan KK, AbuBakar S (2019) Resveratrol affects Zika virus replication in vitro. Sci Rep 9:1–11. https://doi.org/10.1038/s41598-019-50674-3
14. Huang H, Liao D, Zhou G, et al (2020) Antiviral activities of resveratrol against rotavirus in vitro and in vivo. Phytomedicine 77:. https://doi.org/10.1016/j.phymed.2020.153230
15. Yang M, Wei J, Huang T, et al (2020) Resveratrol inhibits the replication of severe acute respiratory syndrome coronavirus 2 (<scp>SARS-CoV</scp> -2) in cultured Vero cells. Phyther Res ptr.6916.

https://doi.org/10.1002/ptr.6916
16. Lin SC, Ho CT, Chuo WH, et al (2017) Effective inhibition of MERS-CoV infection by resveratrol. BMC Infect Dis 17:144. https://doi.org/10.1186/s12879-017-2253-8
17. Dick GWA (1952) Zika Virus (I). Isolations and serological specificity. Trans R Soc Trop Med Hyg 46:509–520. https://doi.org/10.1016/0035-9203(52)90042-4
18. Baud D, Gubler DJ, Schaub B, et al (2017) An update on Zika virus infection. Lancet 390:2099–2109
19. Musso D, Gubler DJ (2016) Zika virus. Clin Microbiol Rev 29:487–524. https://doi.org/10.1128/CMR.00072-15
20. de Oliveira JF, Pescarini JM, de Souza Rodrigues M, et al (2020) The global scientific research response to the public health emergency of Zika virus infection. PLoS One 15:. https://doi.org/10.1371/journal.pone.0229790
21. Pacho MN, Pugni EN, Briyith J, et al (2021) Antiviral activity against Zika virus of a new formulation of curcumin in poly lactic- co -glycolic acid nanoparticles. J Pharm Pharmacol 1–9. https://doi.org/10.1093/jpp/rgaa045
22. Poland GA, Ovsyannikova IG, Kennedy RB (2019) Zika Vaccine Development: Current Status. Mayo Clin Proc 94:2572–2586. https://doi.org/10.1016/j.mayocp.2019.05.016
23. Giovannoni F, Bosch I, Polonio CM, et al (2020) AHR is a Zika virus host factor and a candidate target for antiviral therapy. Nat Neurosci 23:939–951. https://doi.org/10.1038/s41593-020-0664-0
24. Fernando Martínez-Pulgarín D, Miguel Córdoba-Ortega C, Daniel Padilla-Pantoja F (2019) The Eye and the Zika Virus. In: Zika Virus Disease [Working Title]. IntechOpen
25. Roach T, Alcendor DJ (2017) Zika virus infection of cellular components of the blood-retinal barriers: Implications for viral associated congenital ocular disease. J Neuroinflammation 14:. https://doi.org/10.1186/s12974-017-0824-7
26. Ventura C V., Ventura LO (2018) Ophthalmologic manifestations associated with Zika Virus infection. Pediatrics 141:S161–S166. https://doi.org/10.1542/peds.2017-2038E
27. Zhao Z, Yang M, Azar SR, et al (2017) Viral retinopathy in experimental models of zika infection. Investig Ophthalmol Vis Sci 58:4075–4085. https://doi.org/10.1167/iovs.17-22016
28. Singh PK, Guest J-M, Kanwar M, et al (2017) Zika virus infects cells lining the blood-retinal barrier and causes chorioretinal atrophy in mouse eyes. JCI Insight 2:1–14. https://doi.org/10.1172/jci.insight.92340
29. Guevara JG, Agarwal-Sinha S (2018) Ocular abnormalities in congenital Zika syndrome: A case report, and review of the literature. J Med Case Rep 12:. https://doi.org/10.1186/s13256-018-1679-y
30. Simonin Y, Erkilic N, Damodar K, et al (2019) Zika virus induces strong inflammatory responses and impairs homeostasis and function of the human retinal pigment epithelium. EBioMedicine 39:315–331. https://doi.org/10.1016/j.ebiom.2018.12.010
31. Strauss O (2005) The Retinal Pigment Epithelium in Visual Function. https://doi.org/10.1152/physrev.00021.2004.-Located

32. Qin S, Gerard A Rodrigues (2008) Progress and perspectives on the role of RPE cell inflammatory responses in the development of age-related macular degeneration. J Inflamm Res 1:49. https://doi.org/10.2147/jir.s4354
33. Abu-Amero KK, Kondkar AA, Chalam K V. (2016) Resveratrol and ophthalmic diseases. Nutrients
34. García CC, Vázquez CA, Giovannoni F, et al (2020) Cellular Organelles Reorganization During Zika Virus Infection of Human Cells. Front Microbiol 11:1–13. https://doi.org/10.3389/fmicb.2020.01558
35. Alaimo A, Di Santo M, Domínguez Rubio A, et al (2020) Toxic effects of A2E in human ARPE-19 cells were prevented by resveratrol: a potential nutritional bioactive for age-related macular degeneration treatment. Arch Toxicol 94:553–572. https://doi.org/10.1007/s00204-019-02637-w
36. Alaimo A, García Liñares G, Bujjamer JM, et al (2019) Toxicity of blue led light and A2E is associated to mitochondrial dynamics impairment in ARPE-19 cells: implications for age-related macular degeneration. Arch Toxicol 93:1401–1415. https://doi.org/10.1007/s00204-019-02409-6
37. Studer G, Rempfer C, Waterhouse AM, et al (2020) QMEANDisCo—distance constraints applied on model quality estimation. Bioinformatics 36:1765–1771. https://doi.org/10.1093/bioinformatics/btz828
38. Guex N, Peitsch MC, Schwede T (2009) Automated comparative protein structure modeling with SWISS-MODEL and Swiss-PdbViewer: A historical perspective. Electrophoresis 30:. https://doi.org/10.1002/elps.200900140
39. Bienert S, Waterhouse A, De Beer TAP, et al (2017) The SWISS-MODEL Repository-new features and functionality. Nucleic Acids Res 45:D313–D319. https://doi.org/10.1093/nar/gkw1132
40. Bertoni M, Kiefer F, Biasini M, et al (2017) Modeling protein quaternary structure of homo- and hetero-oligomers beyond binary interactions by homology. Sci Rep 7:. https://doi.org/10.1038/s41598-017-09654-8
41. Waterhouse A, Bertoni M, Bienert S, et al (2018) SWISS-MODEL: Homology modelling of protein structures and complexes. Nucleic Acids Res 46:W296–W303. https://doi.org/10.1093/nar/gky427
42. Laskowski RA, MacArthur MW, Moss DS, Thornton JM (1993) PROCHECK: a program to check the stereochemical quality of protein structures. J Appl Crystallogr 26:283–291. https://doi.org/10.1107/s0021889892009944
43. Eisenberg D, Lüthy R, Bowie JU (1997) VERIFY3D: Assessment of protein models with three-dimensional profiles. Methods Enzymol 277:396–404. https://doi.org/10.1016/S0076-6879(97)77022-8
44. Wiederstein M, Sippl MJ (2007) ProSA-web: Interactive web service for the recognition of errors in three-dimensional structures of proteins. Nucleic Acids Res 35:. https://doi.org/10.1093/nar/gkm290
45. Ghosh J, Chowdhury AR, Srinivasan S, et al (2018) Cigarette Smoke Toxins-Induced Mitochondrial Dysfunction and Pancreatitis Involves Aryl Hydrocarbon Receptor Mediated Cyp1 Gene Expression: Protective Effects of Resveratrol. Toxicol Sci 166:428–440. https://doi.org/10.1093/toxsci/kfy206
46. Hanwell MD, Curtis DE, Lonie DC, et al (2012) Avogadro: An advanced semantic chemical editor, visualization, and analysis platform. J Cheminform 4:. https://doi.org/10.1186/1758-2946-4-17

47. Frisch MJ, GW T, HB S, et al (2009) G09 | Gaussian.com. https://gaussian.com/glossary/g09/. Accessed 17 Dec 2020
48. Schaftenaar G, Vlieg E, Vriend G (2017) Molden 2.0: quantum chemistry meets proteins. J Comput Aided Mol Des 31:789–800. https://doi.org/10.1007/s10822-017-0042-5
49. Pettersen EF, Goddard TD, Huang CC, et al (2004) UCSF Chimera - A visualization system for exploratory research and analysis. J Comput Chem 25:1605–1612. https://doi.org/10.1002/jcc.20084
50. Dunn KC, Aotaki-Keen AE, Putkey FR, Hjelmeland LM (1996) ARPE-19, a human retinal pigment epithelial cell line with differentiated properties. Exp Eye Res 62:155–170. https://doi.org/10.1006/exer.1996.0020
51. Rambhatla L, Chiu CP, Glickman RD, Rowe-Rendleman C (2002) In vitro differentiation capacity of telomerase immortalized human RPE cells. Investig Ophthalmol Vis Sci 43:1622–1630
52. Kuznetsova A V., Kurinov AM, Aleksandrova MA (2014) Cell Models to Study Regulation of Cell Transformation in Pathologies of Retinal Pigment Epithelium. J. Ophthalmol. 2014
53. Madreiter-Sokolowski CT, Sokolowski AA, Graier WF (2017) Dosis facit sanitatem—Concentration-dependent effects of resveratrol on mitochondria. Nutrients
54. Giacomello M, Pyakurel A, Glytsou C, Scorrano L (2020) The cell biology of mitochondrial membrane dynamics. Nat Rev Mol Cell Biol 21:204–224. https://doi.org/10.1038/s41580-020-0210-7
55. Khan M, Syed GH, Kim SJ, Siddiqui A (2015) Mitochondrial dynamics and viral infections: A close nexus. Biochim. Biophys. Acta - Mol. Cell Res. 1853:2822–2833
56. Tennen RI, Michishita-Kioi E, Chua KF (2012) Finding a target for resveratrol. Cell 148:387–389
57. Beedanagari SR, Bebenek I, Bui P, Hankinson O (2009) Resveratrol inhibits dioxin-induced expression of human CYP1A1 and CYP1B1 by inhibiting recruitment of the aryl hydrocarbon receptor complex and RNA polymerase II to the regulatory regions of the corresponding genes. Toxicol Sci 110:61–67. https://doi.org/10.1093/toxsci/kfp079
58. Liu WC, Shyu JF, Lin YF, et al (2020) Resveratrol rescue indoxyl sulfate-induced deterioration of osteoblastogenesis via the aryl hydrocarbon receptor /MAPK pathway. Int J Mol Sci 21:1–23. https://doi.org/10.3390/ijms21207483
59. Mohammadi-Bardbori A, Bengtsson J, Rannug U, et al (2012) Quercetin, resveratrol, and curcumin are indirect activators of the aryl hydrocarbon receptor (AHR). Chem Res Toxicol 25:1878–1884. https://doi.org/10.1021/tx300169e
60. Pastorková B, Vrzalová A, Bachleda P, Dvořák Z (2017) Hydroxystilbenes and methoxystilbenes activate human aryl hydrocarbon receptor and induce CYP1A genes in human hepatoma cells and human hepatocytes. Food Chem Toxicol 103:122–132. https://doi.org/10.1016/j.fct.2017.03.008
61. De Medina P, Casper R, Savouret JF, Poirot M (2005) Synthesis and biological properties of new stilbene derivatives of resveratrol as new selective aryl hydrocarbon modulators. J Med Chem 48:287–291. https://doi.org/10.1021/jm0498194

62. Pirola L, Fröjdö S Critical Review Resveratrol: One Molecule, Many Targets. https://doi.org/10.1002/iub.47
63. Saw WG, Pan A, Subramanian Manimekalai MS, Grüber G (2017) Structural features of Zika virus non-structural proteins 3 and -5 and its individual domains in solution as well as insights into NS3 inhibition. Antiviral Res 141:73–90. https://doi.org/10.1016/j.antiviral.2017.02.005
64. Devnarain N, Soliman MES (2019) Molecular mechanism of resveratrol inhibition of Zika virus NS3 helicase: Behind the scenes. Future Virol. 14:73–84
65. Hoffmann HH, Kunz A, Simon VA, et al (2011) Broad-spectrum antiviral that interferes with de novo pyrimidine biosynthesis. Proc Natl Acad Sci U S A 108:5777–5782. https://doi.org/10.1073/pnas.1101143108
66. Mazzucco MB, Talarico LB, Vatansever S, et al (2015) Antiviral activity of an N-allyl acridone against dengue virus. J Biomed Sci 22:. https://doi.org/10.1186/s12929-015-0134-2
67. Sepulveda CS, Fascio ML, Garcia CC, et al (2013) Acridones As Antiviral Agents: Synthesis, Chemical and Biological Properties. Curr Med Chem 20:2402–2414. https://doi.org/10.2174/0929867311320190002
68. Sepúlveda CS, Fascio ML, Mazzucco MB, et al (2008) Synthesis and evaluation of N-substituted acridones as antiviral agents against haemorrhagic fever viruses. Antivir Chem Chemother 19:41–47. https://doi.org/10.1177/095632020801900106
69. Sepúlveda CS, García CC, Fascio ML, et al (2012) Inhibition of Junin virus RNA synthesis by an antiviral acridone derivative. Antiviral Res 93:16–22. https://doi.org/10.1016/j.antiviral.2011.10.007
70. Potter GA, Patterson LH, Wanogho E, et al (2002) The cancer preventative agent resveratrol is converted to the anticancer agent piceatannol by the cytochrome P450 enzyme CYP1b1. Br J Cancer 86:774–778. https://doi.org/10.1038/sj.bjc.6600197
71. Mishra A, Dey S (2019) Molecular Docking Studies of a Cyclic Octapeptide-Cyclosaplin from Sandalwood. https://doi.org/10.20944/preprints201906.0091.v1
72. Levy E, Delvin E, Marcil V, Spahis S (2020) Can phytotherapy with polyphenols serve as a powerful approach for the prevention and therapy tool of novel coronavirus disease 2019 (COVID-19)? Am J Physiol Endocrinol Metab 319:E689–E708. https://doi.org/10.1152/ajpendo.00298.2020
73. Serra D, Almeida LM, Dinis TCP (2018) Dietary polyphenols: A novel strategy to modulate microbiota-gut-brain axis. Trends Food Sci Technol 78:224–233. https://doi.org/10.1016/j.tifs.2018.06.007
74. Brglez Mojzer E, Knez Hrnčič M, Škerget M, et al (2016) Polyphenols: Extraction Methods, Antioxidative Action, Bioavailability and Anticarcinogenic Effects. Molecules 21:. https://doi.org/10.3390/molecules21070901
75. Kubota S, Kurihara T, Ebinuma M, et al (2010) Resveratrol prevents light-induced retinal degeneration via suppressing activator protein-1 activation. Am J Pathol 177:1725–1731. https://doi.org/10.2353/ajpath.2010.100098
76. Jarratt RA, Bartlett H, Eperjesi F (2013) Retinal Effects of Resveratrol. US Ophthalmic Rev 06:132. https://doi.org/10.17925/usor.2013.06.02.132

77. Nashine S, Nesburn AB, Kuppermann BD, Kenney MC (2020) Role of resveratrol in transmitochondrial AMD RPE cells. Nutrients 12:. https://doi.org/10.3390/nu12010159
78. Watkins R, Wu L, Zhang C, et al (2015) Natural product-based nanomedicine: Recent advances and issues. Int J Nanomedicine 10:6055–6074. https://doi.org/10.2147/IJN.S92162
79. Campagna M, Rivas C (2010) Antiviral activity of resveratrol. Biochem. Soc. Trans. 38:50–53
80. Ramdani LH, Bachari K (2020) Potential therapeutic effects of Resveratrol against SARS-CoV-2. Acta Virol 64:276–280. https://doi.org/10.4149/av_2020_309
81. Han YS, Penthala NR, Oliveira M, et al (2017) Identification of resveratrol analogs as potent anti-dengue agents using a cell-based assay. J Med Virol 89:397–407. https://doi.org/10.1002/jmv.24660
82. Tiku V, Tan M-W, Dikic I (2020) Mitochondrial Functions in Infection and Immunity Trends in Cell Biology. Trends Cell Biol 30:. https://doi.org/10.1016/j.tcb.2020.01.006
83. Ren Z, Zhang X, Ding T, et al (2020) Mitochondrial Dynamics Imbalance: A Strategy for Promoting Viral Infection. Front Microbiol 11:. https://doi.org/10.3389/fmicb.2020.01992
84. Yu CY, Liang JJ, Li JK, et al (2015) Dengue Virus Impairs Mitochondrial Fusion by Cleaving Mitofusins. PLoS Pathog 11:. https://doi.org/10.1371/journal.ppat.1005350
85. Chatel-Chaix L, Cortese M, Romero-Brey I, et al (2016) Dengue Virus Perturbs Mitochondrial Morphodynamics to Dampen Innate Immune Responses. Cell Host Microbe 20:342–356. https://doi.org/10.1016/j.chom.2016.07.008
86. Barbier V, Lang D, Valois S, et al (2017) Dengue virus induces mitochondrial elongation through impairment of Drp1-triggered mitochondrial fission. Virology 500:149–160. https://doi.org/10.1016/j.virol.2016.10.022
87. Pannu N, Bhatnagar A (2019) Resveratrol: from enhanced biosynthesis and bioavailability to multitargeting chronic diseases. Biomed Pharmacother 109:2237–2251. https://doi.org/10.1016/j.biopha.2018.11.075
88. Wang N, Luo Z, Jin M, et al (2019) Exploration of age-related mitochondrial dysfunction and the anti-aging effects of resveratrol in zebrafish retina. Aging (Albany NY) 11:3117–3137. https://doi.org/10.18632/aging.101966
89. Zhang X, Feng Y, Wang Y, et al (2018) Resveratrol ameliorates disorders of mitochondrial biogenesis and dynamics in a rat chronic ocular hypertension model. Life Sci 207:234–245. https://doi.org/10.1016/j.lfs.2018.06.010
90. Pang Y, Qin M, Hu P, et al (2020) Resveratrol protects retinal ganglion cells against ischemia induced damage by increasing Opa1 expression. Int J Mol Med 46:1707–1720. https://doi.org/10.3892/ijmm.2020.4711
91. Zimmermann A, Gu JJ, Spychala J, Mitchell BS (1996) Inosine monophosphate dehydrogenase expression: Transcriptional regulation of the type I and type II genes. In: Advances in Enzyme Regulation. Elsevier Ltd, pp 75–84

92. K. Vyas V, Ghate M (2011) Recent Developments in the Medicinal Chemistry and Therapeutic Potential of Dihydroorotate Dehydrogenase (DHODH) Inhibitors. Mini-Reviews Med Chem 11:1039–1055. https://doi.org/10.2174/138955711797247707
93. Munier-Lehmann H, Vidalain PO, Tangy F, Janin YL (2013) On dihydroorotate dehydrogenases and their inhibitors and uses. J. Med. Chem. 56:3148–3167
94. Chung S, Yao H, Caito S, et al (2010) Regulation of SIRT1 in cellular functions: Role of polyphenols. Arch. Biochem. Biophys. 501:79–90
95. Zhou M, Luo J, Zhang H (2018) Role of Sirtuin 1 in the pathogenesis of ocular disease (Review). Int J Mol Med 42:13–20. https://doi.org/10.3892/ijmm.2018.3623
96. Yang T, Li S, Zhang X, et al (2015) Resveratrol, sirtuins, and viruses. Rev Med Virol 25:431–445. https://doi.org/10.1002/rmv.1858

Tables

Table 1. Comparison of binding energies of RES and known ligands with the selected proteins.

Protein	Ligand	Binding energy (kcal/mol)
CYP1B1	Resveratrol	-7.79
AHR	2,3,7,8-tetrachlorodibenzodioxin	-8.36
	CH-223191	-9.21
	Resveratrol	-7.42
DHODH	4,5-Dihydroorotic acid	-8.35
	Resveratrol	-8.15
GMPR2	Guanosine monophosphate	-6.59
	Resveratrol	-7.65
RdRp	Adenosine Triphosphate	-6.77
	Resveratrol	-7.45

Table 2. Amino acids interaction with the natural ligands and RES. Amino acids that interact with RES and the known ligand are shown in bold.

Protein		H-bond interactions	Hydrofobic contact
CYP1B1	RES	Asn265, Asn228, Gln332	Phe231, Leu264, Phe268, Gly329, Ala330, Asp333, Thr334, Ile399, Leu509 and the HEM group.
AHR	TCDD	-	**Phe16**, **Thr18**, His20, Cys29, **Leu37**, **Tyr39**, **Leu44**, Phe53, His66, **Leu82**, **Val110**, **Gln112**.
	RES	**Tyr39**, Gly50, **Gln112**.	**Phe16**, **Thr18**, **His20, Cys29**, Gly33, Arg34, **Leu37**, **Leu44**, **Leu82**, **Val110**.
DHODH	DHO	**Ala96**, Ser120, Asn212, **Lys255**, **Thr283**, **Asn284**, Gly334, **Gly335**, **Tyr356**, **Thr357.**	Ala95, Gly97, Gly119, Asn145, Thr285, Ser305, Leu309, **Val333**, Gln354, Leu355.
	RES	**Ala96**, **Thr283**, Val336	**Lys255**, **Asn284**, Gly306, **Val333**, **Gly335**, Ser337, Leu355, **Tyr356**, **Thr357,** Ala358.
GMPR2	GMP	Ala131, Gly179, Asp219	Asp129, Asn158, **Gly220**, Ile180, Gly181, Pro182, **Cys186**, Thr188.
	RES	Cys222, Met240, Met269	Met55, Gly183, Ser184, Val185, **Cys186**, **Gly220**, Gly221, Leu241, Gly242, Gly243 Gly268.
RdRp	ATP	Arg731, **Tyr768**, **Thr795**, **Thr796**, Trp797, **Ser798**	**Leu513**, **Leu736**, **Arg739**, **Met763**, **Leu767**, **His800**, **Gly801**, Trp805
	RES	**Leu736**, **Ser798**, **His800**	**Leu513**, **Arg739**, Ala740, Tyr760, **Met763**, Trp764, **Leu767**, **Tyr768**, **Thr795**, **Thr796**, **Gly801**.

Figures

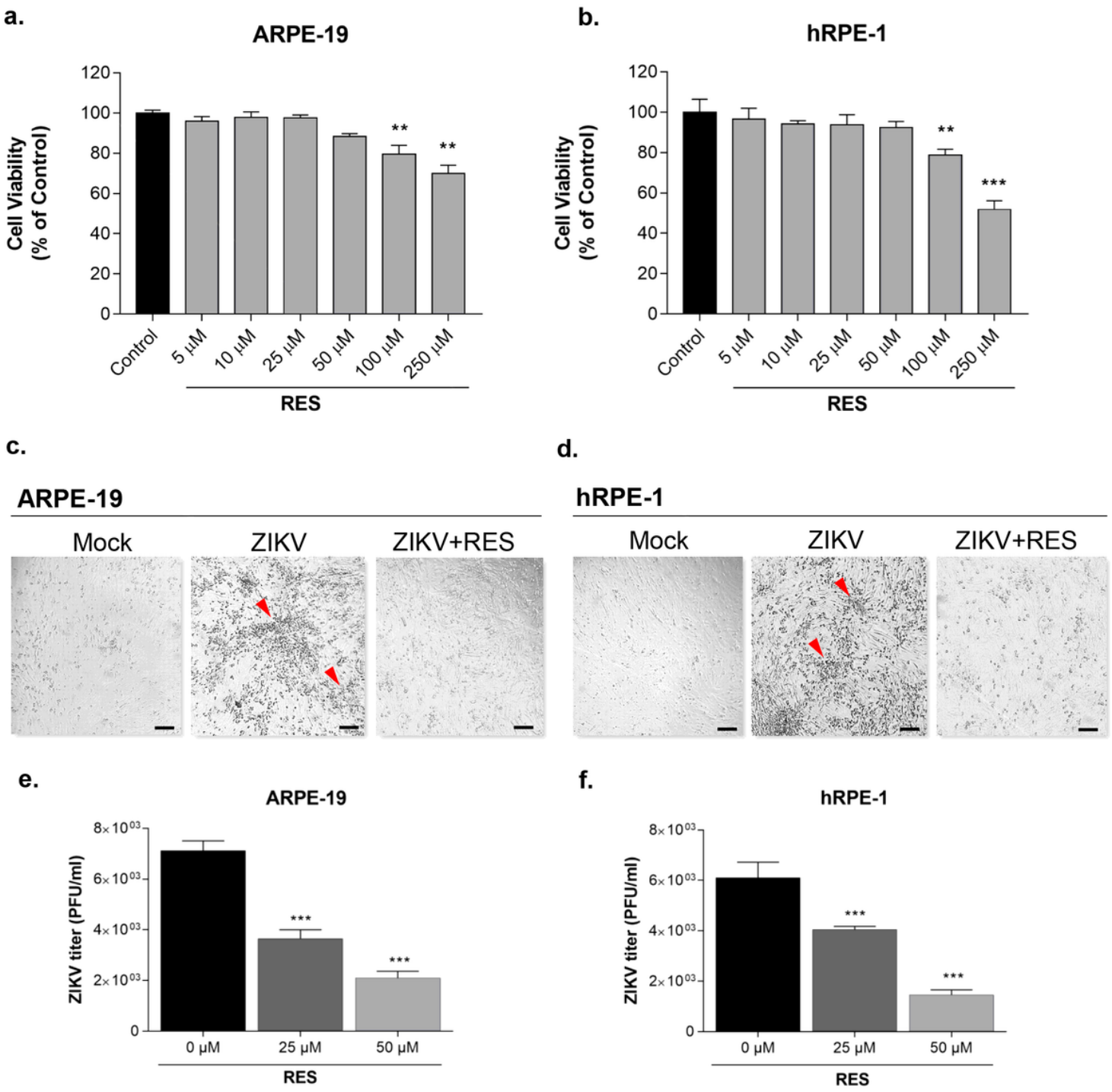

Figure 1

Effect of RES on ZIKV-infected RPE cells Determination of the ARPE-19 (a) and hRPE-1 (b) cell viability. The cells were incubated with different concentrations of RES dissolved in EtOH / PBS. The viability of the cells was determined by the MTT assay. Data were expressed as a percentage of viable cells compared to control (mean ± SEM). ZIKV and RES effect on cellular morphology in ARPE-19 (c) and hRPE-1 (d). Analysis of cell morphology by phase contrast microscopy of RPE cells mock-infected (first column), ZIKV-infected (second column) or ZIKV-infected and treated with 50 µM RES (third column). The photographs were obtained at 48 hpi (Magnification: 10 X; scale bar: 50 µm). Cells presenting cytopathic

effect (red arrows). Quantification of the viral yield. Cell cultures of ARPE-19 (e) or hRPE-1 (f) were infected with ZIKV (moi=0.5) and cultured in the presence or absence of 25 μM or 50 μM RES. The supernatants of the cultures were harvested at 48 h pi and the viral titer was determined by standard plaque assay (PFU/ml). The statistical analysis by one-way ANOVA with Newman-Keuls post-tests. ** p <0.01; *** p <0.001 vs control.

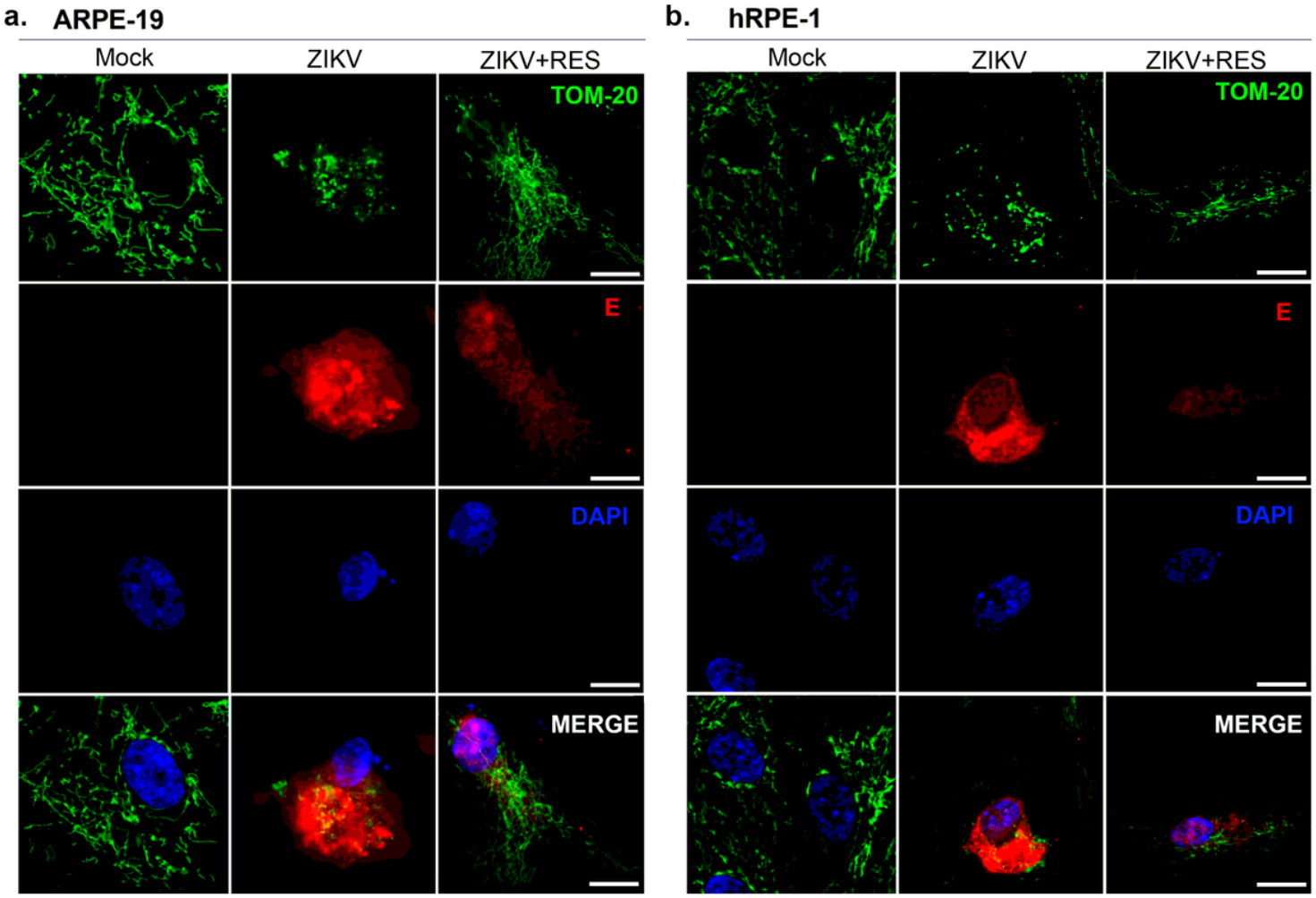

Figure 2

Effect of RES on mitochondrial morphology of ZIKV-infected RPE cells Cell cultures of ARPE-19 (a) or hRPE-1 (b) were mock-infected (first column) or infected with ZIKV (moi = 0.5) and cultured in the absence (second column) or presence (third column) of 50 μM RES. After 48 h, the cells were fixed and then stained against a mitochondrial protein (TOM-20), ZIKV envelope protein (E) and the nuclei (DAPI). The samples were visualized through epifluorescence microscopy. Magnification 60 X; scale bar: 10 μm.

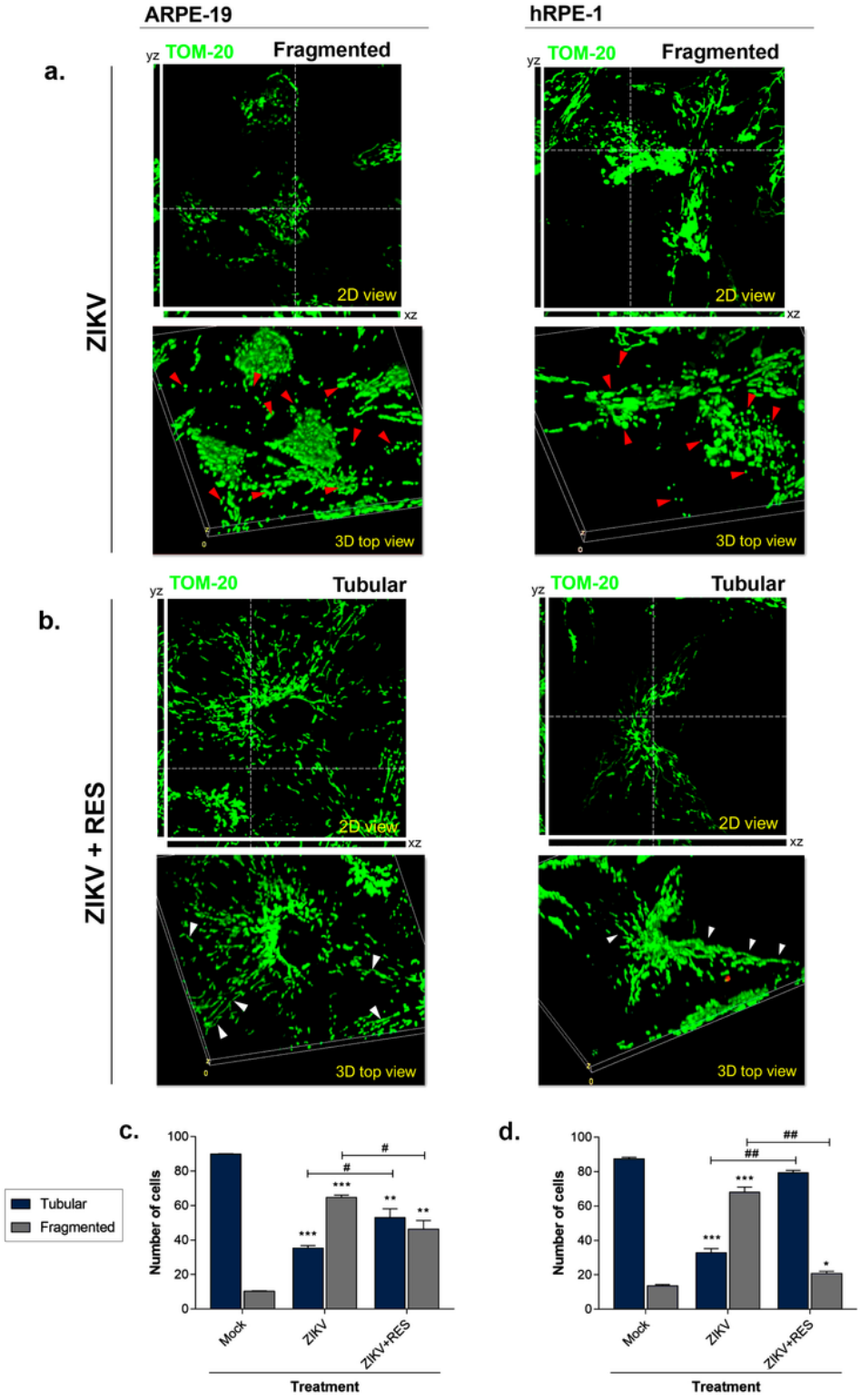

Figure 3

Study of the mitochondrial dynamics z-stacks representative images from confocal microscopy used for 3D reconstruction; the crosshairs show the xz and yz planes. The images correspond to ZIKV-infected (a) ARPE-19 (left column) and hRPE-1 (right column) cells culture samples or ZIKV-infected and RES-treated (b) ARPE-19 (left column) and hRPE-1 (right column) cells. Different mitochondrial morphologies are indicated. White arrows: m. tubular; red arrows: m. fragmented and swollen. Scale bar: 10 μm.

Quantification of mitochondrial morphologies of ARPE-19 cells (c) or hRPE-1 (d) cells. 100 cells per treatment were counted, and it was determined and plotted the number of cells with distinct mitochondrial morphologies (tubular or fragmented) for each treatment. The statistical analysis was performed through one-way ANOVA * p <0.05; ## p <0.01; *** p <0.001 vs control.

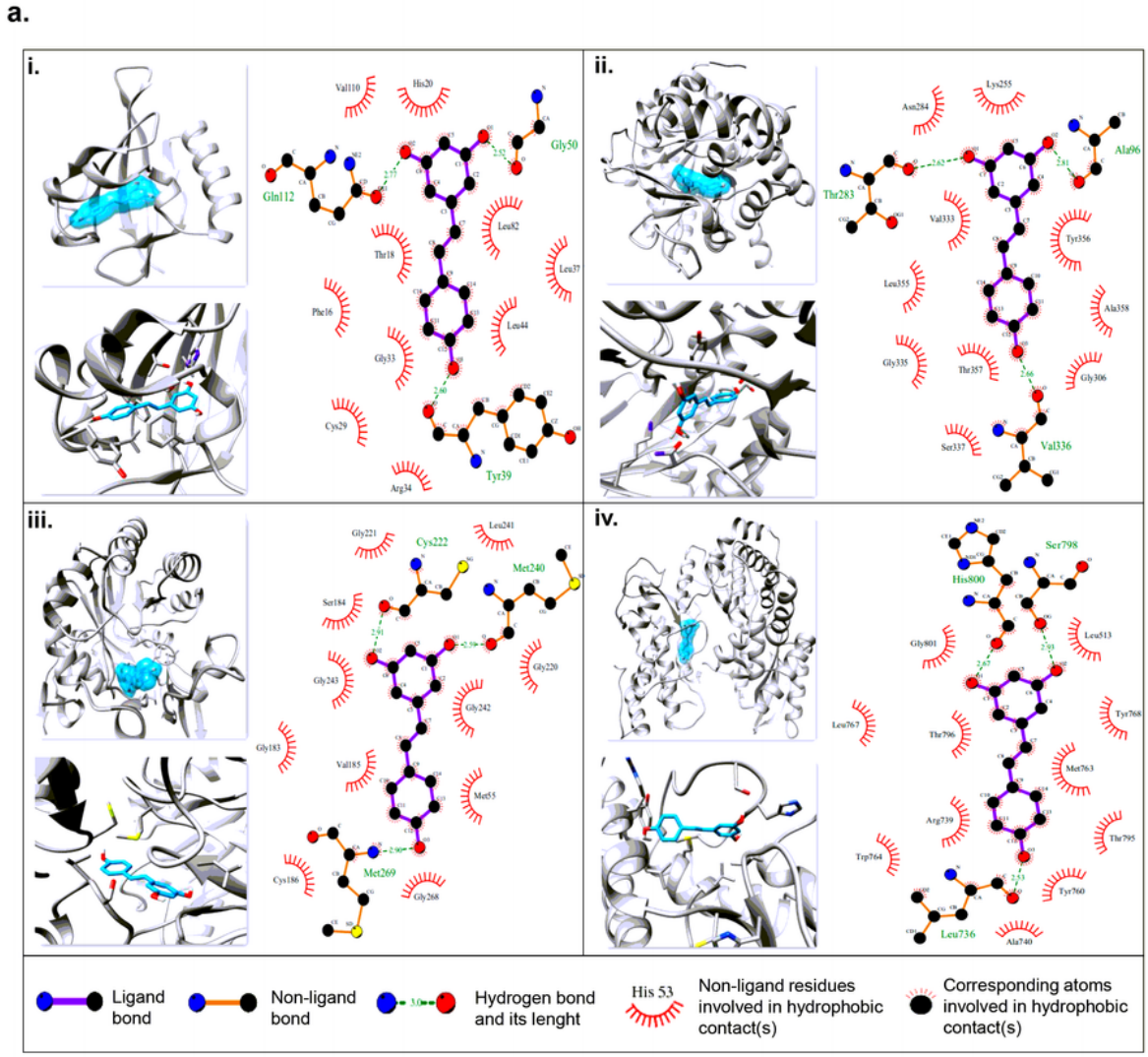

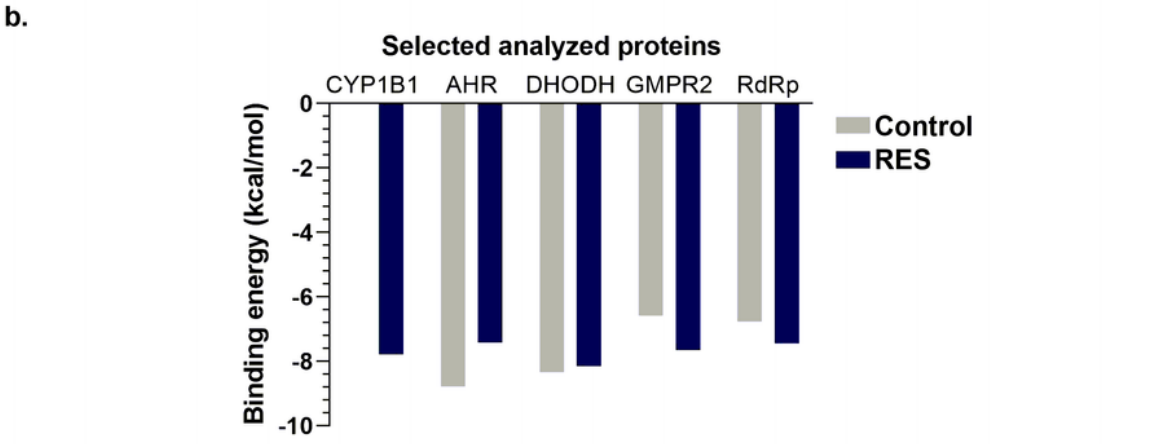

Figure 4

Molecular docking of RES with the selected targets (a) Molecular interactions of RES with (i) AHR (ii) DHODH (iii) GMPR2 (iv) RdRp. The 3D structures of the complexes are visualized with UCSF Chimera and the 2D interactions with LigPlot+ v.2.1. In the 3D images, the surface and the structure of RES are represented in cyan color. The proteins are graphed as gray ribbons. (b) Binding energies of the different proteins with RES and the control ligands. Controls: TCDD for AHR, 4,5-Dihydroorotic acid (DHO) for DHODH, guanosine monophosphate (GMP) for GMPR2 and adenosine triphosphate (ATP) for RdRp. CYP1B1 is the reference protein.

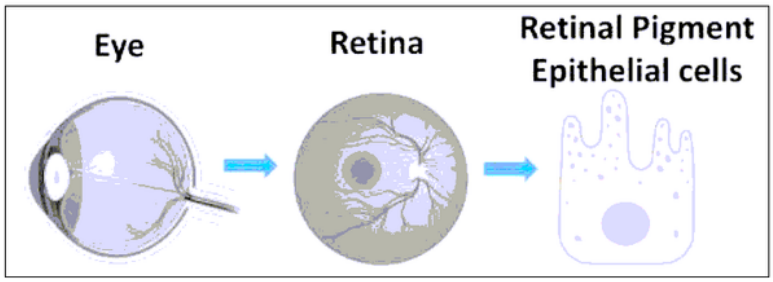

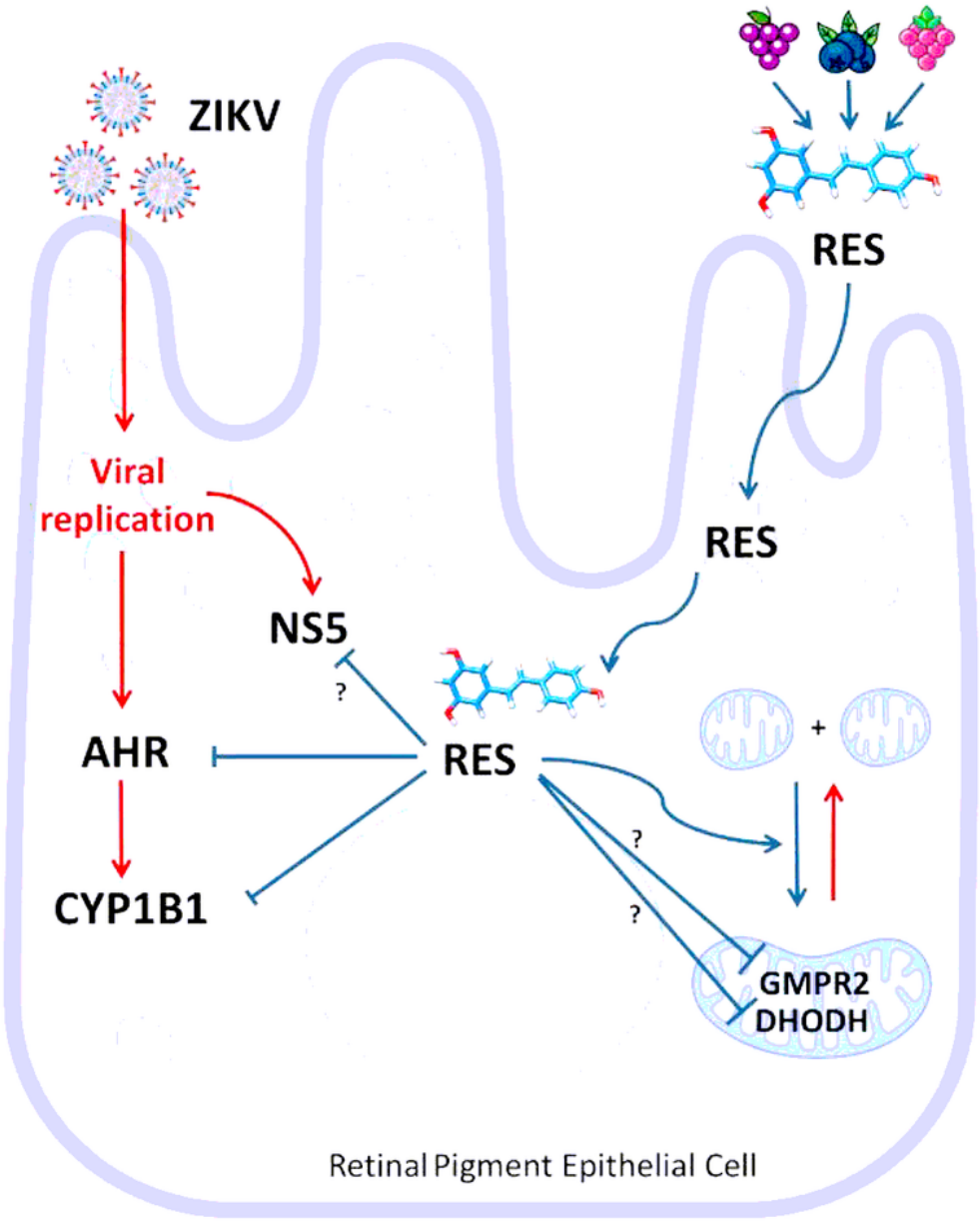

Figure 5

Proposed scheme describing the protective role of RES against Zika infection in human RPE cells.

Supplementary Files

This is a list of supplementary files associated with this preprint. Click to download.

- GraphicalAbstract.tif